THE JOURNAL OF PHYSICAL CHEMISTRY Letters

Letter

pubs.acs.org/JPCL

Water-Induced Decoupling of Tracer and Electrochemical Oxygen Exchange Kinetics on Mixed Conducting Electrodes

Andreas Nenning,[†] Edvinas Navickas,[†] Herbert Hutter, and Jürgen Fleig*

Institute of Chemical Technologies and Analytics, Vienna University of Technology, Getreidemarkt 9, Vienna, A-1060, Austria

Supporting Information

ABSTRACT: Isotope exchange depth profiling and electrochemical impedance spectroscopy are usually regarded as complementary tools for measuring the surface oxygen exchange activity of mixed conducting oxides, for example used in solid oxide fuel cell (SOFC) electrodes. Only very few studies compared electrical (k^q) and tracer (k^*) exchange coefficients of solid−gas interfaces measured under identical conditions. The 1:1 correlation between k^q and k^* often made is thus more an assumption than experimentally verified. In this study it is shown that the measured rates of electrical and tracer exchange of oxygen may strongly differ. Simultaneous acquisition of k^q and k^* on $La_{0.6}Sr_{0.4}FeO_{3-\delta}$ and $SrTi_{0.3}Fe_{0.7}O_{3-\delta}$ thin film electrodes revealed that $k^* > 100\ k^q$ in humid oxidizing ($^{16}O_2$ + $H_2{}^{18}O$) and humid reducing (H_2 + $H_2{}^{18}O$) atmospheres. These results are explained by fast water adsorption and dissociation on surface oxygen vacancies, forming two surface hydroxyl groups. Hence, interpreting experimentally determined k^* values in terms of electrochemically relevant oxygen exchange is not straightforward.

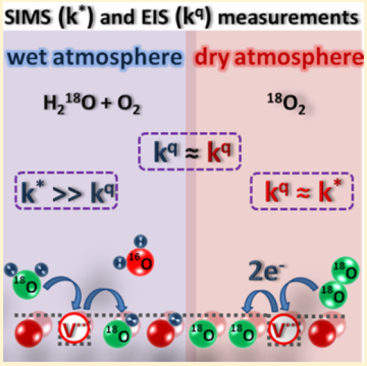

Mixed ionic and electronic conductors (MIECs) are frequently applied on the oxygen side of solid oxide fuel/electrolysis cells (SOFC/SOEC), and some of them, for example $La_{0.6}Sr_{0.4}FeO_{3-\delta}$ and $SrTi_{0.3}Fe_{0.7}O_{3-\delta}$, are even candidates for both SOFC/SOEC fuel side electrodes as well as oxygen electrodes. In such electrochemical cells oxygen is either incorporated from the gas phase into the MIEC or released from the MIEC into the atmosphere. This kind of electrochemical surface reaction can be expressed by

$$O_{atm} + V_O^{\cdot\cdot} + 2e' \leftrightarrow O_O^{\times} \quad (1)$$

Essentially, this is a redox reaction which includes transfer of electrons. The oxygen in the gas O_{atm} may either be present as O_2 molecule or in form of H_2O, in the latter case hydrogen is produced or consumed in the surface reaction. In equilibrium, both forward and backward reaction of eq 1 take place at the same rate and thus without any net current. An oxygen exchange coefficient can be used in order to quantify the kinetics of such a reaction in dynamic equilibrium. This oxygen exchange coefficient is often determined by electrochemical impedance spectroscopy (EIS).[1−4] Using a small AC voltage, a small perturbation of the equilibrium is introduced and thus a net current can be measured. EIS thus yields an area specific resistance (ASR) of the electrochemical surface reaction (reaction 1) and an electrical oxygen exchange coefficient (k^q) can then be calculated by the relation[5,6]

$$k^q = \frac{k_b T}{(ze)^2 c_o \mathrm{ASR}} \quad (2)$$

Symbol c_O denotes the oxide ion concentration, z is the charge number (−2 for oxygen ions) and k_b, T, and e are Boltzmanns constant, temperature, and elementary charge, respectively.

Another common method for analyzing the oxygen exchange kinetics of MIECs is ^{18}O isotope exchange and depth profiling (IEDP), yielding a tracer exchange coefficient (k^*). Generally, those experiments take place by exposing the MIEC to tracer enriched gas and as long as no voltage is applied during the experiment the net flux of oxygen across the surface remains zero. Upon tracer incorporation ^{16}O and ^{18}O atoms swap their positions between oxide ($O_O^{\times}$) and atmosphere (O_{atm}) according to the reaction

$$^{18}O_{atm} + {}^{16}O_O^{\times} \rightarrow {}^{18}O_O^{\times} + {}^{16}O_{atm} \quad (3)$$

The net ^{18}O incorporation flux and thus also ^{16}O release flux of this reaction (in oxygen atoms/cm^{2}s) depends on the fraction of ^{18}O ($f(^{18}O)$) in the gas and at the oxide surface by

$$j_O^* = c_O k^* (f(^{18}O)_{atm} - f(^{18}O)_{oxidesurface}) \quad (4)$$

In principle, the two oxygen exchange reactions (reactions 3 and 1) may take place by different atomistic mechanisms. Only if the two reaction parts of ^{18}O incorporation and ^{16}O release in eq 3 can be identified as incorporation and release of an oxygen atom by means of reaction 1, the coefficients k^* and k^q are identical (or at least similar since a small difference due to correlation effects as for diffusion coefficients may still remain).[6] This requires the ^{18}O incorporation and the ^{16}O release in eq 3 to be locally unrelated and to include a change of the oxygen reduction state, i.e., an electron transfer. Hence, in

Received: April 12, 2016
Accepted: July 8, 2016

DOI: 10.1021/acs.jpclett.6b00778
J. Phys. Chem. Lett. 2016, 7, 2826−2831

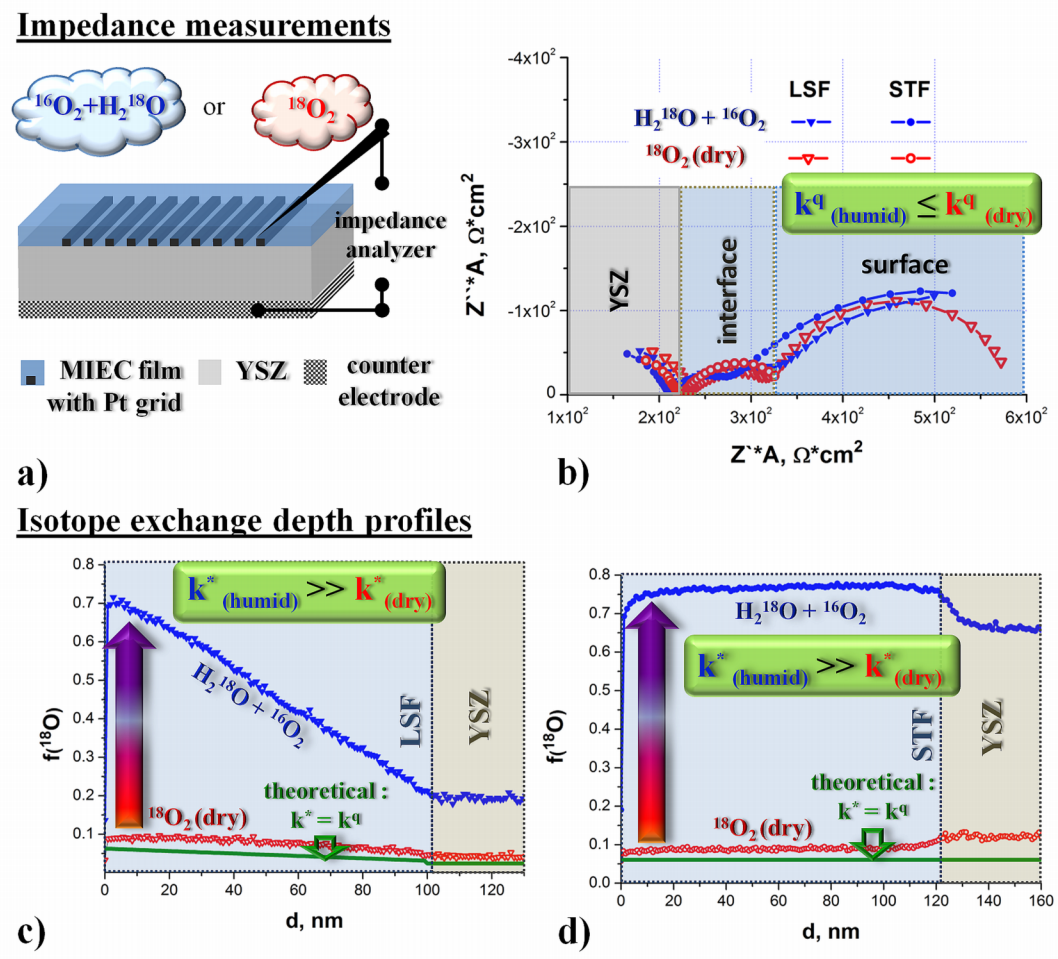

Figure 1. (a) Sketch of sample geometry and tracer exchange routine during EIS. (b) Impedance measurements on $La_{0.6}Sr_{0.4}FeO_{3-\delta}$ (LSF) and $SrTi_{0.3}Fe_{0.7}O_{3-\delta}$ (STF) thin film electrodes during tracer exchange in dry and humid oxidizing atmosphere at 418 °C, normalized to the active electrode area. (c,d) ^{18}O tracer depth profiles in LSF and STF measured after the exchange, including a simulation assuming $k^* = k^q_{dry}$ (theoretical).

principle, the corresponding k factors of tracer and EIS experiments can be rather different as already pointed out in ref 6.

Despite this possibility of strongly different k^* and k^q values, their equality is assumed in most cases and only very few studies compared the two coefficients obtained upon identical experimental conditions. Similar values of k^* and k^q were indeed found for $La_{0.6}Sr_{0.4}CoO_{3-\delta}$ at 400 °C[7] in dry O_2, indicating that the exchange mechanism as well as its rate limiting step is identical in both types of experiments. Some studies showed much faster tracer exchange in humidified ($H_2{}^{18}O$) atmosphere, e.g., on $La_2Mo_2O_9$,[8,9] $(Ce,Gd)O_{2-\delta}$, and $(Zr,Y)O_{2-\delta}$,[10,11] and $BaTiO_3$.[12] In refs 11, 13, and 14 strongly increased tracer exchange kinetics and slightly faster electrochemical kinetics on Pt-YSZ electrodes in humid atmospheres were attributed to fast water dissociation on the oxide surface. Increased gas phase ^{18}O exchange kinetics were observed on $(La,Sr)MnO_{3-\delta}$ (LSM) and $(La,Sr)(Co,Fe)O_{3-\delta}$ (LSCF) by the introduction of water and related to dissociation of water.[15] From ambient pressure XPS measurements[16] on $(Ce,Sm)O_{2-\delta}$ in $H_2 + H_2O$ atmosphere, fast water dissociation on surface oxygen vacancies is assumed as well. However, these studies only rely on indirect observations, because the individual rates of electrically driven oxygen exchange and water dissociation on the surface were not quantified and correlated for identical conditions.

Accordingly, there remains the question under which conditions k^* gives a meaningful measure of the kinetics of the electrochemical oxygen exchange according to reaction 1. In the experiments presented here, k^* and k^q are simultaneously determined on one and the same electrode. Impedance spectroscopy was performed during isotope exchange in various ^{18}O containing atmospheres on different mixed conducting oxides. Hence, quantitative comparison of the exchange coefficients k^* and k^q became possible. Partly very severe differences with $k^* > 100k^q$ are found, particularly in humid atmosphere, and a mechanistic explanation is provided.

$La_{0.6}Sr_{0.4}FeO_{3-\delta}$ and $SrTi_{0.3}Fe_{0.7}O_{3-\delta}$ thin film model electrodes with an embedded Pt grid as electronic current collector were prepared on yttria stabilized zirconia (YSZ) single crystals with porous LSF counter electrodes. Impedance spectra were acquired during ^{18}O tracer exchange at 396−418 °C, as sketched in Figure 1a. These tracer exchange experiments lasted 10−20 min. Please note that in these experiments the tracer incorporation still corresponds to oxygen tracer exchange without field since the isotope exchange reaction 3 is not significantly influenced by the small AC voltage of 10 mV. EIS is only required to determine k^q in addition to k^*. Four different atmospheres were used for tracer exchange: (1) 200

DOI: 10.1021/acs.jpclett.6b00778
J. Phys. Chem. Lett. 2016, 7, 2826−2831

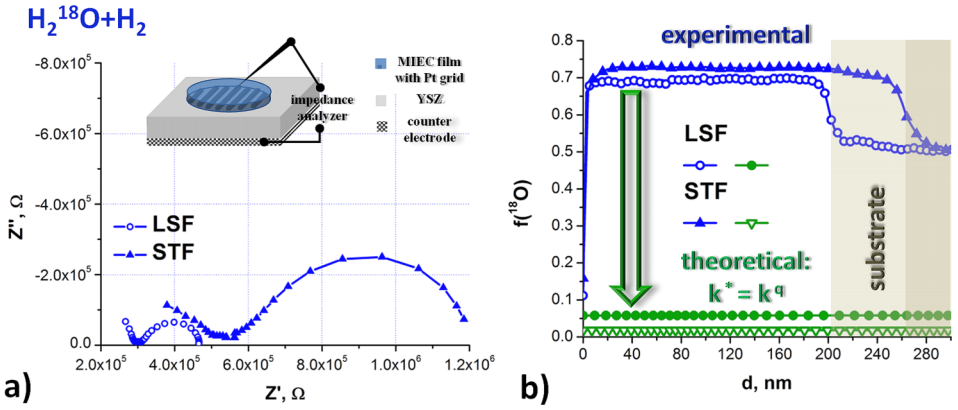

Figure 2. (a) Impedance measurements on LSF and STF thin films microelectrodes during isotope exchange in humid reducing atmosphere at 396 °C. (b) Measured ^{18}O depth profiles, including a simulation assuming $k^* = k^q$ (theoretical).

Table 1. Tracer (k^*) and Electrical (k^q) Exchange Coefficients of $La_{0.6}Sr_{0.4}FeO_{3-\delta}$ and $SrTi_{0.3}Fe_{0.7}O_{3-\delta}$ in Various Atmospheres[a]

material	dry oxidizing 418 °C	usual oxidizing 418 °C	humid oxidizing 418 °C	humid reducing 396 °C
LSF	$k^* = 1.3 \times 10^{-8}$ cm s^{-1}	$k^* = 1.5 \times 10^{-8}$ cm s^{-1}	$k^* = 1.5 \times 10^{-6}$ cm s^{-1}	$k^* = 2.5 \times 10^{-6}$ cm s^{-1}
	$k^q = 8.5 \times 10^{-9}$ cm s^{-1}	$k^q = 3.1 \times 10^{-9}$ cm s^{-1}	$k^q = 5.9 \times 10^{-9}$ cm s^{-1}	$k^q = 1.8 \times 10^{-8}$ cm s^{-1}
			($k^*_{min} = 4.5 \times 10^{-7}$ cm s^{-1})	($k^*_{min} = 7.5 \times 10^{-7}$ cm s^{-1})
	$k^*/k^q = 1.5$	$k^*/k^q = 4.8$	$k^*/k^q = 254$ (>76)	$k^*/k^q = 139$ (>42)
STF	$k^* = 3.0 \times 10^{-8}$ cm s^{-1}	$k^* = 3.5 \times 10^{-8}$ cm s^{-1}	$k^* = 5.0 \times 10^{-6}$ cm s^{-1}	$k^* = 4.3 \times 10^{-6}$ cm s^{-1}
	$k^q = 1.9 \times 10^{-8}$ cm s^{-1}	$k^q = 5.9 \times 10^{-9}$ cm s^{-1}	$k^q = 5.0 \times 10^{-9}$ cm s^{-1}	$k^q = 5.0 \times 10^{-9}$ cm s^{-1}
			($k^*_{min} = 1.2 \times 10^{-6}$ cm s^{-1})	($k^*_{min} = 8.3 \times 10^{-7}$ cm s^{-1})
	$k^*/k^q = 1.6$	$k^*/k^q = 5.9$	$k^*/k^q = 1000$ (>240)	$k^*/k^q = 860$ (>166)

[a]For humid oxidizing and humid reducing conditions, a minimum k^*_{min} is also included, representing the k^* in the case of the highest possible $H_2{}^{18}O$ fraction of 97.1%. This leads to the k^*/k_q ratio given in parentheses, e.g., (>76).

mbar $^{18}O_2$, dried through a zeolite filter (dry oxidizing); (2) bottled $^{18}O_2$ without drying step (usual oxidizing); (3) 200 mbar $^{16}O_2$ humidified with $H_2{}^{18}O$ (humid oxidizing); and (4) 25 mbar H_2 in Ar, humidified with $H_2{}^{18}O$ (humid reducing). Water vapor pressures in humid gases were 15−25 mbar. After the tracer exchange, the samples were quenched with a rate of ∼150 °C/min and ^{18}O depth profiles were acquired by secondary ion mass spectrometry (SIMS). Experimental details on the preparation and design of the electrodes, the tracer exchange procedure and the SIMS analysis are provided in the Supporting Information.

The acquired impedance spectra (Figures 1b and 2a) show the onset of a high frequency arc and one or two arcs at intermediate and low frequencies. This is very typical for mixed conducting thin film electrodes and often reported in literature for similar systems, see, e.g., 2−4 and 17−19. In accordance with those earlier studies the following interpretation is made: The high frequency arc is primarily caused by the ohmic drop in the electrolyte (here YSZ) but may also include a contribution from a contact resistance. The arcs at intermediate and low frequencies can be attributed to the electrochemical electrode reactions. For MIEC thin film electrodes three reaction steps have to be distinguished: electrochemical oxygen exchange reaction (cf. eq 1), transport of oxide ions across the thin film and ion transfer between electrode and electrolyte. For materials with moderate to high ionic conductivity, and thus also in our case, ion transport across the thin layer does not significantly contribute to the overall electrode resistance.

Interpretation of the two arcs is made on the basis of the associated capacitances. The large capacitance of several mF/cm^2 found for all low frequency semicircles can only be explained by the high chemical bulk capacitance[2,19] of the electrode. According to the equivalent circuit model for mixed conducting materials introduced in ref 20, the corresponding parallel resistor has then to be the resistance of the electrochemical surface reaction (in the absence of ionic transport limitation). The smaller intermediate frequency arc, on the other hand, is most probably caused by an interfacial ion transfer barrier, but also the counter electrode may contribute.[2,17,18] As it was done in many earlier studies from different groups, the area-specific resistance of the surface reaction (ASR) was thus determined by fitting the low frequency semicircle to a parallel resistor and a constant phase element[3,4,17,18,21,22] and normalizing the resistance to the active electrode area. Electrical exchange coefficients (k^q) were calculated from the ASR using eq 2, and all values are summarized in Table 1. Interestingly, in all atmospheres and for both materials, the ASR is in the range of 200 Ω·cm^2 ($k^q \approx 8 \times 10^{-9}$ cm/s), and differences are far less than 1 order of magnitude. This is also in line with the literature data of STF extrapolated to 420 °C.[4] Some effects of humidity on the ASR were already reported in the literature[23−25] at higher temperatures and are also found in this study (see Supporting Information).

In Figures 1c,d and 2b, depth profiles of the ^{18}O isotope fraction $f(^{18}O)$ are shown for dry and humid oxidizing as well as humid reducing exchange conditions. All profiles were calculated from raw data by restricting the in-plane integration of the ^{18}O signals to MIEC regions without the ion blocking platinum current collector beneath. Most of the depth profiles are flat within the MIEC film and some exhibit a distinct step at the MIEC|YSZ interface. Only for LSF in oxidizing conditions (Figure 1c) a clear slope can be observed, indicating low ionic conductivity. This is caused by the small amount of oxygen

DOI: 10.1021/acs.jpclett.6b00778
J. Phys. Chem. Lett. 2016, 7, 2826−2831

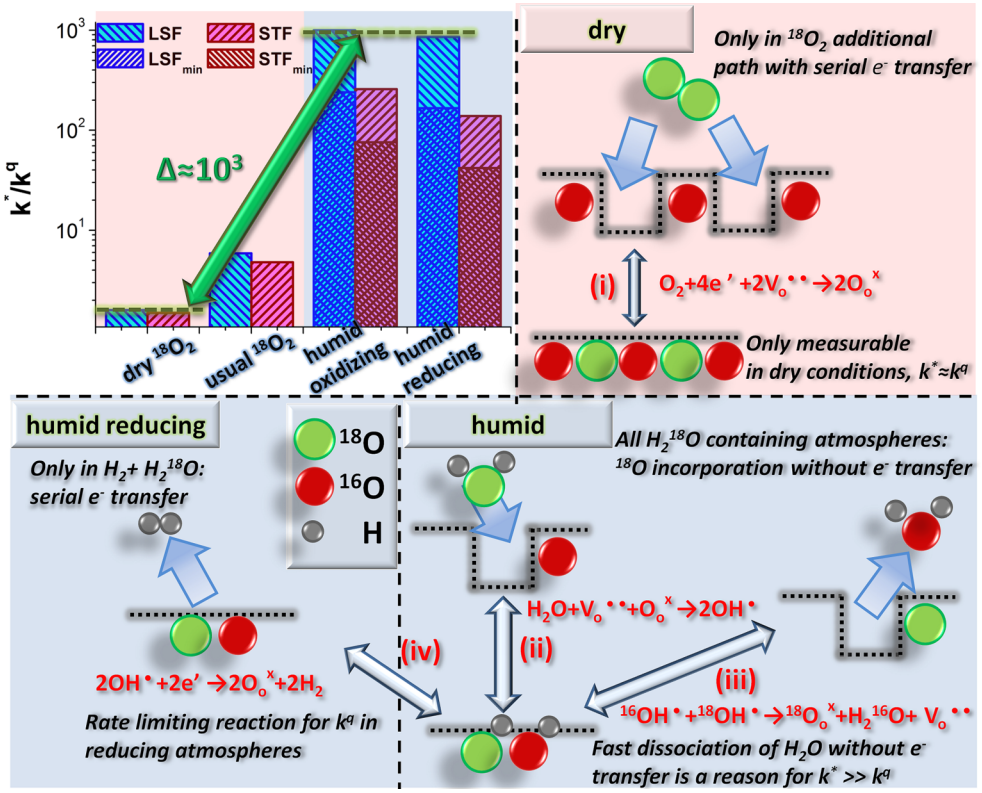

Figure 3. Ratios of k^*/k^q from Table 1 are shown in the bar graph. In addition the minimum ratios of k^*/k^q in humid reducing and humid oxidizing atmospheres are also included (LSF_{min} and STF_{min}). The sketches show different oxygen incorporation mechanisms in $^{18}O_2$ (top) and $H_2{}^{18}O$ atmosphere (bottom). Reaction 1 shows the $^{18}O_2$ incorporation into surface vacancies, requiring an electron transfer. This dominates only in dry atmosphere. In $H_2{}^{18}O$ containing atmospheres $H_2{}^{18}O$ can adsorb on a surface vacancy and dissociate into two OH^- groups (reaction step ii). $^{18}O^{2-}$ is then formed by desorption of $H_2{}^{16}O$, using a neighboring ^{16}O ion (reaction step iii). In H_2 containing atmospheres also H_2 formation from two surface hydroxyls through a redox reaction step (iv) may follow reaction step ii.

vacancies of LSF in oxidizing atmosphere, especially at lower temperatures ($\delta \approx 0.0001$ at 418 °C[26]). For STF in oxidizing and reducing conditions, but also for LSF in reducing conditions, the oxygen vacancy concentration and thus the ionic conductivity is rather high.[26,27] In all humidified atmospheres, the tracer fraction is even close to the atmospheric fraction of $H_2{}^{18}O$ (see below).

These profiles were fitted using finite element simulations, considering isotope exchange (k^*) and diffusion (D^*) coefficients of the MIEC and an interfacial transfer coefficient at the MIEC|YSZ interface (k^*_{int}). Reasons for the slight upward step found for STF in dry air are unknown yet and this was not taken into account. In the simulation, D^* of YSZ was fixed to the value calculated from the measured ionic conductivity of YSZ using Nernst−Einsteiǹs relation, i.e., to 2.1×10^{-8} cm^2/s at 418 °C and 1.0×10^{-8} cm/s^2 at 396 °C. The atmospheric ^{18}O concentration of 97.1% (provided by the supplier) was assumed in dry oxidizing conditions, whereas a concentration of 80% and 77% $H_2{}^{18}O$ was estimated for humid oxidizing and humid reducing conditions, respectively, by evaluating the ^{18}O concentration found in the MIEC on top of the ion blocking Pt layer (not shown). In humid conditions, this value of the isotope fraction in the heated gas atmosphere is critical for the k^* calculation, due to the high ^{18}O concentrations in the samples, and thus k^* values are prone to errors. Hence, a very conservative estimate of the minimum k^* was also made by considering the maximum $H_2{}^{18}O$ level in the atmosphere as defined for $^{18}O_2$ by the provider (97.1%). Those minimal k^* values are also given in Table 1. An upper limit of k^* cannot be given on the basis of the present data, but any k^* value larger than the given ones would be in agreement with all conclusions anyway.

A reasonable D^* value of the MIEC could be only determined for LSF in oxidizing atmosphere and the following discussion is limited to k^* values. Those are summarized in Table 1. Simulated profiles assuming $k^* = k^q{}_{dry}$ are also shown in Figure 1 and Figure 2 (theoretical).

Please note that the surface exchange kinetics of thin film electrodes may vary from sample to sample and also due to degradation. Therefore, the main information is revealed by the ratio of k^*/k^q obtained on one and the same electrode at exactly the same time. The ratios of k factors in all four atmospheres are summarized in Table 1 and in the bar graph of Figure 3. In dry oxidizing atmosphere, reasonable agreement of k^* and k^q is found, even though k^* is slightly higher than k^q. This may have several reasons: The tremendous increase of k^* in humid atmospheres (see below) suggests that even traces of residual humidity may enhance k^*. The increase of the k^*/k^q ratio found upon removal of the zeolite filter is an indication for this effect (see "usual oxidizing" column in Table 1 and Figure 3). Moreover, the ASR of the surface reaction (eq 1) may be overestimated since other processes (e.g., in-plane charge transport[28]) might increase the size of the electrode arc, leading to slightly underestimated k^q values.

In humidified oxidizing atmosphere, the electrode ASR slightly increases, which somewhat decreases k^q, while the tracer surface exchange coefficient k^* becomes 2 to 3 orders of magnitude larger than k^q for LSF and STF. This large difference

DOI: 10.1021/acs.jpclett.6b00778
J. Phys. Chem. Lett. 2016, 7, 2826−2831

strongly indicates existence of different mechanisms of electrically measured oxygen exchange (EIS) and tracer oxygen exchange, in particular since $H_2{}^{18}O$ is the only source of oxygen tracer; $H_2{}^{18}O$ does not directly contribute to the reaction of eq 1 and thus to k^q. A decoupling of k^* and k^q can be expected in the presence of an isotope exchange mechanism that does not change oxygen reduction states. Such a process contributes to k^* but not to k^q. A likely nonredox reaction is the fast adsorption and dissociation of $H_2{}^{18}O$ on a surface oxygen vacancy, forming two hydroxyl groups (reaction step ii in Figure 3). Here, the oxidation states of O and H remain −2 and +1, respectively. A fast rate of this process is assumed on YSZ[13,14] and ceria surfaces in reducing conditions.[6] The subsequent desorption of $H_2{}^{16}O$ using a neighboring $^{16}O^{2-}$ ion (reaction step iii in Figure 3) can then finalize a tracer exchange according to eq 3 without any electron transfer. Hence, we propose that this nonredox oxygen exchange by water dissociation leads to the strongly enhanced tracer exchange coefficient in $H_2{}^{18}O$.

These results are of high relevance for tracer exchange experiments in O_2 atmosphere as they highlight the importance of having absolutely water-free gas during an isotope exchange experiment. Even traces of $H_2{}^{18}O$-based humidity can lead to accelerated tracer exchange that, however, does not imply increased performance as an SOFC electrode. Such traces of $H_2{}^{18}O$ may easily be present in bottled $^{18}O_2$ gas since some residual H_2 is typically found in bottled $^{18}O_2$ (25 ppm according to the manufacturer used here). This H_2 most probably forms $H_2{}^{18}O$ at exchange temperatures. Also higher levels of $H_2{}^{16}O$ can be very detrimental since this may remove ^{18}O from the solid without electron transfer and thus may lower the measured k^* value and may cause an underestimation of the electrochemical oxygen exchange rate of eq 1.

Reducing H_2 + $H_2{}^{18}O$ atmosphere inevitably contains water, so only one ratio of k^*/k^q is measurable. Also this ratio is very large (>100, see Table 1), and thus we conclude that k^* is again not a meaningful measure for describing the electrochemical exchange kinetics by means of eq 1. As discussed for humid oxidizing atmosphere, also here very fast tracer oxygen exchange is possible through water dissociation by reaction steps ii and iii in Figure 3, which are not redox reactions. The much slower electrical oxygen exchange also requires the formation of H_2 and electron transfer to surface OH groups by the redox reaction iv in Figure 3. The very large difference between k^* and k^q in reducing atmosphere therefore suggests that an electron transfer or the formation of H_2 from surface hydroxyl groups is rate limiting on LSF and STF hydrogen electrodes, as already assumed for ceria.[16]

Accordingly, under reducing conditions the very fast tracer exchange still gives valuable mechanistic information on the electrochemical reaction. If water dissociation (reaction ii, Figure 3) was rate limiting in the overall water splitting reaction ($H_2O + V_O^{\cdot\cdot} \rightarrow H_2 + O_O^{\times} + 2e'$), the H_2 desorption reaction (reaction step iv, Figure 3) would be faster than the desorption of $H_2{}^{16}O$ (reaction step iii, Figure 3), and the isotope exchange reaction would primarily take place by the reaction involving the electron transfer. Consequently, an agreement of k^q and k^* would result; $k^q \approx k^*$ would thus imply water dissociation to be rate limiting.

Our experiments revealed by direct measurement of reaction rates that this is not at all the case ($k^* > 100\ k^q$). Accordingly, we conclude that the rate of water dissociation (hydroxyl formation) and water desorption is much faster than the hydrogen reduction and desorption steps. Therefore, either the charge transfer from the oxide to a surface hydroxyl or the formation of H_2 from two hydroxyl groups is rate-limiting. Methodologically, this means that tracer exchange experiments cannot deliver reliable information on the electrochemical oxygen exchange kinetics when humidity is present in the atmosphere. In such a case, one cannot obtain meaningful estimates of electrical exchange rates from measured k^* values, since moving to dry conditions, as for O_2, is not an option with H_2 being involved.

The absolute k^* values in humid reducing and humid oxidizing conditions are very similar, which further indicates that tracer is exchanged through the same mechanism. Interestingly, k^q values found in oxidizing and reducing conditions are also very similar. However, this is most likely a coincidence without mechanistic reason behind because strongly different activation energies of the O_2 reduction[4] and water splitting reaction[28] are found, e.g., on STF. It is also important to note that all experimental results were obtained in the temperature range of about 400 °C and the behavior may be different at the usually much higher operation temperatures of SOFC electrodes.

■ ASSOCIATED CONTENT

Supporting Information

The Supporting Information is available free of charge on the ACS Publications website at DOI: 10.1021/acs.jpclett.6b00778.

Experimental methods including sample preparation, details on heavy water preparation and parameters of ToF-SIMS measurements (PDF)

■ AUTHOR INFORMATION

Corresponding Author

*Tel: +43 (0) 1 58801 15800; Fax: +43 (0) 1 58801 15899; E-mail: j.fleig@tuwien.ac.at.

Author Contributions

†A. Nenning and E. Navickas contributed equally to this work.

Notes

The authors declare no competing financial interest.

■ ACKNOWLEDGMENTS

This work was supported by Austrian Science Fund (FWF) (Projects: F4509-N16 and W1243-N16).

■ REFERENCES

(1) Lai, W.; Haile, S. M. Impedance Spectroscopy as a Tool for Chemical and Electrochemical Analysis of Mixed Conductors: a Case Study of Ceria. *J. Am. Ceram. Soc.* **2005**, *88*, 2979−2997.

(2) Baumann, F. S.; Fleig, J.; Habermeier, H.-U.; Maier, J. Impedance Spectroscopic Study on Well-Defined (La, Sr) (Co, Fe)$O_{3-\delta}$ Model Electrodes. *Solid State Ionics* **2006**, *177*, 1071−1081.

(3) Baumann, F.; Maier, J.; Fleig, J. The Polarization Resistance of Mixed Conducting SOFC Cathodes: A Comparative Study Using Thin Film Model Electrodes. *Solid State Ionics* **2008**, *179*, 1198−1204.

(4) Jung, W. C.; Tuller, H. L. A New Model Describing Solid Oxide Fuel Cell Cathode Kinetics: Model Thin Film $SrTi_{1-x}Fe_xO_{3-\delta}$ Mixed Conducting Oxides−a Case Study. *Adv. Energy Mater.* **2011**, *1*, 1184−1191.

(5) Maier, J. *Physical Chemistry of Ionic Materials: Ions and Electrons in Solids*; Wiley: Chichester, U.K., 2004.

(6) Maier, J. On the Correlation of Macroscopic and Microscopic Rate Constants in Solid State Chemistry. *Solid State Ionics* **1998**, *112*, 197−228.

DOI: 10.1021/acs.jpclett.6b00778
J. Phys. Chem. Lett. 2016, 7, 2826−2831

(7) Kubicek, M.; Huber, T. M.; Welzl, A.; Penn, A.; Rupp, G. M.; Bernardi, J.; Stöger-Pollach, M.; Hutter, H.; Fleig, J. Electrochemical Properties of $La_{0.6}Sr_{0.4}CoO_{3-\delta}$ Thin Films Investigated by Complementary Impedance Spectroscopy and Isotope Exchange Depth Profiling. *Solid State Ionics* **2014**, *256*, 38−44.
(8) Georges, S.; Skinner, S. J.; Lacorre, P.; Steil, M. C. Oxide Ion Diffusion in Optimised LAMOX Materials. *Dalton Trans.* **2004**, 3101−3105.
(9) Liu, J.; Chater, R.; Morris, R. J.; Skinner, S. Oxygen Surface Exchange and Diffusion Studies of $La_2Mo_2O_9$ in Different Exchange Atmospheres. *Solid State Ionics* **2011**, *189*, 39−44.
(10) Sakai, N.; Yamaji, K.; Horita, T.; Xiong, Y. P.; Kishimoto, H.; Brito, M. E.; Yokokawa, H. Effect of Water on Electrochemical Oxygen Reduction at the Interface Between Fluorite-Type Oxide-Ion Conductors and Various Types of Electrodes. *Solid State Ionics* **2004**, *174*, 103−109.
(11) Pietrowski, M.; De Souza, R.; Fartmann, M.; ter Veen, R.; Martin, M. Oxygen Isotope Transport Properties of Yttria-Stabilized Zirconia (YSZ) in O_2-and H_2O-Containing Atmospheres. *Fuel Cells* **2013**, *13*, 673−681.
(12) Kessel, M.; De Souza, R.; Yoo, H.; Martin, M. Strongly Enhanced Incorporation of Oxygen into Barium Titanate Based Multilayer Ceramic Capacitors Using Water Vapor. *Appl. Phys. Lett.* **2010**, *97*, 021910.
(13) Sakai, N.; Yamaji, K.; Horita, T.; Xiong, Y. P.; Kishimoto, H.; Yokokawa, H. Effect of Water on Oxygen Transport Properties on Electrolyte Surface in SOFCs I. Surface Reaction Mechanism of Oxygen Isotope Exchange on Solid Oxide Electrolytes. *J. Electrochem. Soc.* **2003**, *150*, A689−A694.
(14) Sakai, N.; Yamaji, K.; Horita, T.; Kishimoto, H.; Xiong, Y.; Yokokawa, H. Significant Effect of Water on Surface Reaction and Related Electrochemical Properties of Mixed Conducting Oxides. *Solid State Ionics* **2004**, *175*, 387−391.
(15) Huang, Y.-L.; Pellegrinelli, C.; Wachsman, E. D. Fundamental Impact of Humidity on SOFC Cathode Degradation. *ECS Trans.* **2015**, *68*, 699−712.
(16) Feng, Z. A.; El Gabaly, F.; Ye, X.; Shen, Z.-X.; Chueh, W. C. Fast Vacancy-Mediated Oxygen Ion Incorporation Across the Ceria−Gas Electrochemical Interface. *Nat. Commun.* **2014**, *5*, 4374.
(17) Kogler, S.; Nenning, A.; Rupp, G. M.; Opitz, A. K.; Fleig, J. Comparison of Electrochemical Properties of $La_{0.6}Sr_{0.4}FeO_{3-\delta}$ Thin Film Electrodes: Oxidizing vs. Reducing Conditions. *J. Electrochem. Soc.* **2015**, *162*, F317−F326.
(18) Baumann, F.; Fleig, J.; Cristiani, G.; Stuhlhofer, B.; Habermeier, H.-U.; Maier, J. Quantitative Comparison of Mixed Conducting SOFC Cathode Materials by Means of Thin Film Model Electrodes. *J. Electrochem. Soc.* **2007**, *154*, B931−B941.
(19) Jung, W. C.; Tuller, H. L. Impedance Study of $SrTi_{1-x}Fe_xO_{3-\delta}$(x= 0.05 to 0.80) Mixed Ionic-Electronic Conducting Model Cathode. *Solid State Ionics* **2009**, *180*, 843−847.
(20) Jamnik, J.; Maier, J. Generalised Equivalent Circuits for Mass and Charge Transport: Chemical Capacitance and Its Implications. *Phys. Chem. Chem. Phys.* **2001**, *3*, 1668−1678.
(21) Chueh, W. C.; Hao, Y.; Jung, W.; Haile, S. M. High Electrochemical Activity of the Oxide Phase in Model Ceria−Pt and Ceria−Ni Composite Anodes. *Nat. Mater.* **2012**, *11*, 155−161.
(22) Rupp, G. M.; Schmid, A.; Nenning, A.; Fleig, J. The Superior Properties of $La_{0.6}Ba_{0.4}CoO_{3-\delta}$ Thin Film Electrodes for Oxygen Exchange in Comparison to $La_{0.6}Sr_{0.4}CoO_{3-\delta}$. *J. Electrochem. Soc.* **2016**, *163*, F564−F573.
(23) Bucher, E.; Sitte, W.; Klauser, F.; Bertel, E. Oxygen Exchange Kinetics of $La_{0.58}Sr_{0.4}Co_{0.2}Fe_{0.8}O_3$ at 600° C in Dry and Humid Atmospheres. *Solid State Ionics* **2011**, *191*, 61−67.
(24) Simner, S. P.; Anderson, M. D.; Engelhard, M. H.; Stevenson, J. W. Degradation Mechanisms of La−Sr−Co−Fe−O_3 SOFC Cathodes. *Electrochem. Solid-State Lett.* **2006**, *9*, A478−A481.
(25) Simner, S. P.; Anderson, M. D.; Pederson, L. R.; Stevenson, J. W. Performance Variability of La(Sr)FeO_3 SOFC Cathode with Pt, Ag, and Au Current Collectors. *J. Electrochem. Soc.* **2005**, *152*, A1851−A1859.
(26) Kuhn, M.; Hashimoto, S.; Sato, K.; Yashiro, K.; Mizusaki, J. Oxygen Nonstoichiometry, Thermo-Chemical Stability and Lattice Expansion of $La_{0.6}Sr_{0.4}FeO_{3-\delta}$. *Solid State Ionics* **2011**, *195*, 7−15.
(27) Kuhn, M.; Kim, J. J.; Bishop, S. R.; Tuller, H. L. Oxygen Nonstoichiometry and Defect Chemistry of Perovskite-Structured $BaxSr_{1-x}Ti_{1-y}FeyO_{3-y/2+\delta}$ Solid Solutions. *Chem. Mater.* **2013**, *25*, 2970−2975.
(28) Nenning, A.; Opitz, A. K.; Huber, T. M.; Fleig, J. A Novel Approach for Analyzing Electrochemical Properties of Mixed Conducting Solid Oxide Fuel Cell Anode Materials by Impedance Spectroscopy. *Phys. Chem. Chem. Phys.* **2014**, *16*, 22321−22336.

DOI: 10.1021/acs.jpclett.6b00778
J. Phys. Chem. Lett. 2016, 7, 2826−2831